Activation of different MEMS resonant modes with Pulsed Digital Oscillators

Manuel Dominguez-Pumar[a], Elena Blokhina[b], Joan Pons-Nin[a], Orla Feely[b], Jose Luis Sanchez-Rojas[c]

[a]Universitat Politècnica de Catalunya, Barcelona, Spain;

[b]University College Dublin, Dublin, Ireland;

[c]Universidad de Castilla-la-Mancha, Ciudad Real, Spain;

Abstract

The objective of this work is to show that it is possible to excite different vibration modes of MEMS resonators using Pulsed Digital Oscillators. This class of circuits exhibit two different behaviours: the oscillation and the anti-oscillation mode. In the oscillation mode, the oscillator in average provides energy to the resonator, whereas in the anti-oscillation mode, it extracts energy of the resonator until a limit cyucle is reached near the origin. It will be shown that by preparing suitable PDO configurations it is possible to selectively excite different resonant modes of a MEMS resonator. The experimental corroboration has been obtained with a scanning Doppler vibrometer.

1 Introduction

Microcantilevers put into resonance have been extensively used in a variety of applications such as gravimetric sensors, gyroscopes, AFM probes, etc. In gravimetric sensors, the ability to detect small quantities of targeted materials provides a constant challenge in sensing technology and techniques for improving sensitivity of vibrating microresonators are object of many researches. For instance, parametric resonance amplification is an example of an efficient technique [1] that allows the excitation of the same mechanical structure at a higher frequency to improve sensitivity. An alternative way of ultrasensitive mass detection is the use of mode localization in the vibrations of two nearly identical coupled cantilevers [2]. In addition, the selective activation of different spatial vibration modes of a mechanical resonator is reported to be a technique to improve performance for a large number of cantilever-based sensors [3, 4, 5]. Therefore, a technique that can excite the mechanical structure in higher modes may be the object of interest in many specific applications.

Most oscillators use the small signal model of these structures to obtain self-sustained oscillations on MEMS resonators. On the other hand, Pulsed Digital Oscillators (briefly PDOs [6, 7, 8, 9]) are simple circuits that allow to obtain these self-sustained oscillations with an automatic analog to digital conversion. As it can be seen in Figure 1, the main structure contains the MEMS resonator (input port: force, output port: position or velocity), a 1-bit quantizer (sign function) and a feedback filter. These are sampled circuits, and at each sampling time it is only necessary to know whether the resonator is above or below its rest position. The excitation is composed of short pulses of force, and are generated from the previous position samples. The output of the circuit is the bitstream at the output of the quantizer.

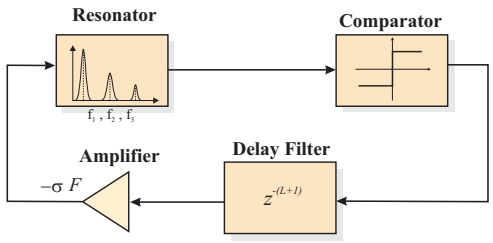

Figure 1: General single feedback topology of the pulsed digital oscillator.

For a given configuration of the oscillator (i.e., a sampling frequency, and a feedback filter) the oscillator may in average either provide energy to the resonator (oscillator mode), or extract energy from it until a limit cycle is reached near the origin (anti-oscillator mode). If the resonator presents two or more resonances, it is possible to excite one of them, by selecting a feedback filter and samping frequency such that for this frequency the oscillator is in the oscillator mode, whereas the others lie in the anti-oscillation region. This will be the mechanism used in this work to excite any given resonance in a

ISBN 978-3-8007-3260-9

MEMS resonator.

2 Analysis of a resonator with multiple vibration modes

The purpose of this section is to obtain a model that allows an easy computation of the system dynamics in the case when the resonator can be excited with more than one resonance. In order to do this, we will begin by analyzing the different vibration modes arising from an equation governing the dynamics of elastic beams (the Euler's equation). From this equation, we will obtain the different resonant modes and from them the iterative model.

2.1 Vibration modes of elastic beams

We consider the micromechanical resonator in the form of a clamped-free beam shown in fig. 2. Transversal deflections of the beam under the external force $F(\xi,\tau)$ are governed by the Euler's equation. The dimensionless equation and the boundary conditions that describe the transverse vibrations of the beam are as follows:

$$\frac{\partial^4 u}{\partial \xi^4} + \frac{\partial^2 u}{\partial \tau^2} + \gamma \frac{\partial u}{\partial \tau} = F(\xi,\tau)\,, \tag{1}$$

$$u(0,\tau) = \frac{\partial u(0,\tau)}{\partial \xi} = 0\,, \qquad \frac{\partial^2 u(1,\tau)}{\partial \xi^2} = \frac{\partial^3 u(1,\tau)}{\partial \xi^3} = 0\,, \tag{2}$$

where $u(\xi,\tau)$ is the transverse displacement at the position ξ and time τ. In (1), the dimensionless coordinate along the beam axis ξ, time τ and the dissipation parameter due to viscous damping γ are defined through the dimensional ones z, t and c:

$$\xi = z/l\,, \qquad \tau = \frac{t}{l^2}\sqrt{\frac{EI}{\rho A}}\,, \qquad \gamma = \frac{cl^2}{\sqrt{\rho A E I}}\,, \tag{3}$$

where E is the Young's modulus, I is the moment of inertia of the cross-section (for beams with a rectangular cross-section $I = bh^3/12$), ρ is the density, A is the area of the cross-section, c is the dissipation coefficient, l is the length of the beam, b is its width and h is its thickness.

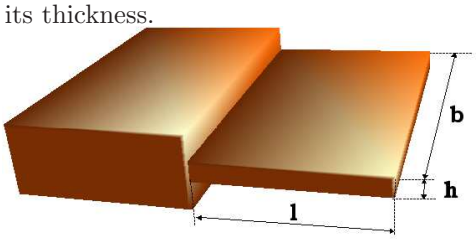

Figure 2: Drawing of a MEMS cantilever similar to those later measured with PDOs..

The continuous equation (1) can be discretized by using a truncated set of linear mode shapes:

$$u(\xi,\tau) = \sum_{i=1}^{M} x_i(\tau)\psi_i(\xi) \tag{4}$$

where $x_i(\tau)$ are time dependent functions and $\psi_i(\xi)$ are the spatial mode shapes. Substituting the latter expression into the equation, multiplying it by ψ_j and integrating over the beam domain, we obtain a system of ordinary differential equations

$$\ddot{x_i} + \gamma \dot{x_i} + \Omega_i^4 x_i = F_i(\tau), \qquad i = 1,\ldots,M\,, \tag{5}$$

which provides the time dependence of the different spatial modes. The frequencies Ω_i^2 are roots of the equation $\cos\Omega_i \cosh\Omega_i = -1$. In the right part of (5), the functions $F_i(\tau)$ define portions of the external force that are transmitted into each mode:

$$F_i(\tau) = \int_0^1 \psi_i(\xi) F(\xi,\tau) d\xi \tag{6}$$

As a result, we obtain that the time evolution of each spatial mode of an elastic beam is governed by the set (5), and that the force transmitted into a given mode depends on the form of the spatial mode shape and the point at which the force is applied.

2.2 PDO iterative map with multiple resonances

In the previous section, we have shown that vibration modes have different time dependencies defined by the set of ordinary differential equations. Every time when excitation is applied to the beam, every mode is excited with a different portion of the driving force. The sensed total position is now can be presented as a sum of all excited modes weighted by some coefficients. In this section we introduce a set of iterative maps to encode the position and velocity of each mode.

The examined system is subjected to pulse excitation in the following form:

$$F(\xi,\tau) = \\ = -\sigma F_0 \sum_n \mathrm{sign}(u(\xi_s,\tau_{n-L-1}))\delta(\xi-\xi_a)\delta(\tau-\tau_n)\,, \tag{7}$$

where $L+1$ is the number of delays in the feedback (see Figure 1), $\tau_n = nT_s$ is the instants of time at which we apply the force pulse, $T_s = 1/f_s$ are the dimensionless time between two impulses, $\delta(x)$ is the Dirac delta function and $\mathrm{sign}(x)$ is the signum function. In this expression, ξ_s is the point of the microcantilever at which the sensing system measures the resonator position and ξ_a is the point at which

the actuating system applies the external driving in order to maintain the oscillations.

If we define the sequence $\{x_{i,n}, v_{i,n}\} = \{x_i(\tau_n), dx_i(\tau_n)/d\tau\}$, that is the sequence of the sampled position and velocity taken from the mass-spring-damper equations (5) for each ith spatial mode, we will be able to formulate iterative equations that describe the dynamics of the system in terms of the complex variables $u_{i,n} = x_{i,n} - jv_{i,n}$:

$$u_{i,n+1} = p_i u_{i,n} - j\zeta_i b_{n-L}\,, \tag{8}$$

$$b_n = \operatorname{sgn} \sum_i \beta_i \mathrm{Re}(u_{i,n})\,, \tag{9}$$

where the coefficients in the retrieve map can be written through the coefficients of the set (5): $p_i = \alpha_i \exp(-j2\pi f_i)$, $\alpha_i = \exp((-2\pi\rho_i f_i)/(\sqrt{1-\rho_i^2}))$, $\rho_i = \gamma/(2\Omega_i^2)$ (the normalised dissipation parameter), $f_i = \Omega_i^2\sqrt{1-\rho_i^2}/f_s$ (the normalised frequency), $\zeta_i = \sigma F_0 \psi(\xi_a)/(\Omega_i^2\sqrt{1-\rho_i^2})$ (the normalized force applied on each mode). The coefficients $\beta_i = \psi_i(\xi_s)/\psi_1(\xi_s)$ depend on the geometry of each mode and the spatial application of the force.

3 Activation of different vibration modes

In this section, we present results based on numerical simulations of the map (8) that show the activation of different modes. First, we consider a resonator with only one resonant frequency. Once a PDO is configured, i.e., the sampling frequency and feedback filters have been specified, two different behaviours may be observed generally:

- *Oscillation mode*: In this mode, the oscillator tends to increase the energy stored in the resonator, until a stable oscillation is obtained of a given amplitude, depending among others parameters on the damping losses.

- *Anti-oscillation or reverse mode*: In this mode, the oscillator is in average always extracting energy of the resonator until a limit cycle is reached near the origin.

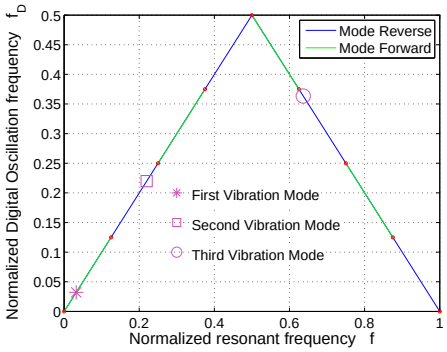

Figure 3: The configuration with L=4, $\sigma = 1$ activates the first resonance of the elastic beam.

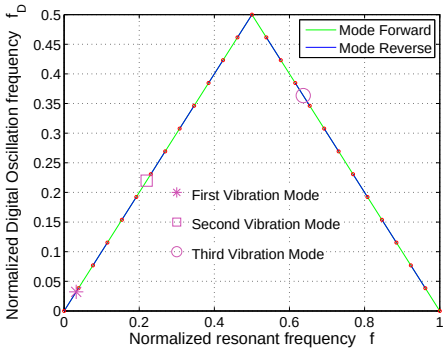

Figure 4: The configuration with L=13, $\sigma = 1$ activates the first resonance of the elastic beam.

It has been shown in [10] that for feedback delay filters of the form $G(z) = z^{L+1}$ and $\sigma = 1$, the oscillation regions are of the form: $\langle f(L+1)\rangle \leq 0.5$, where the $\langle\cdot\rangle$ is the modulus one operation, and f is the normalized frequency. In order to force oscillations of a given resonant mode, the strategy consists on finding a feedback filter (L, σ), such that the normalized resonant frequency lies in an oscillation segment, and all the other in anti-oscillation segments. In order to commute to another resonant mode, another pair of (L', σ') must be found, such that it is this mode the only one located in the oscillation region.

It can be seen in Figures 3-4, examples of two different PDO configurations to activate successively the first two resonances of an elastic beam. In the case when two or more modes are in oscillation regimes, the output of the PDO depends on the initial conditions (initial deformation of the cantilever). The system is capable of selective excitation of various spatial modes of the mechanical structure in the feedback loop. The location of the sensing/actuation system may enhance high-order modes and improve the sensitivity of the device.

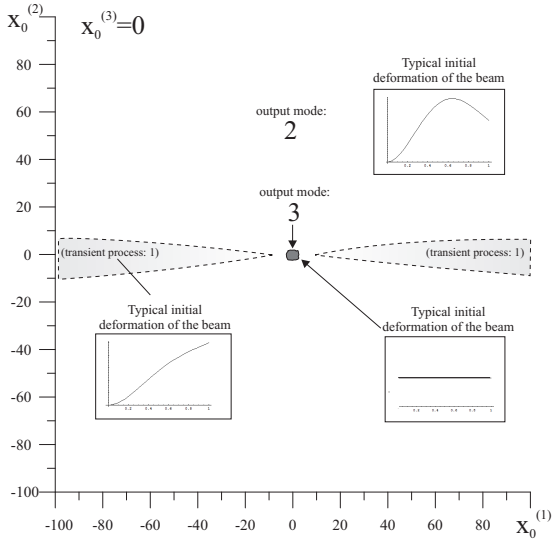

Figure 5: Plane of initial conditions (x_0^1, x_0^2) showing the possible output of the resonator. $\gamma = 0.001$, $f_1 = 0.1845$, $\xi_s = \xi_a = 0.3$. The gray areas outlined by dashed lines are the areas with extremely long transient processes (up to 10^5 iterations) when the system displays first oscillations of the first spatial mode and converge eventually to oscillations that correspond to the third mode.

4 Experimental results

The objective of this section is to show the experimental results obtained with a MEMS cantilever with thermoelectric actuation and piezoresistive sensing, using the approach proposed previously to excite different its first three resonant modes. This device has been used previously and its main characteristics can be found in [7].

4.1 Characterization of the mechanical resonances of the MEMS cantilever

In order to prepare different PDO configurations to excite the different vibration modes of the MEMS cantilever, it was first carried out the characterization of the different modes of the mechanical structure. Using a Polytec MSV 400 laser Doppler vibrometer, the mechanical spectrum of the device has been obtained (see Figure 6).

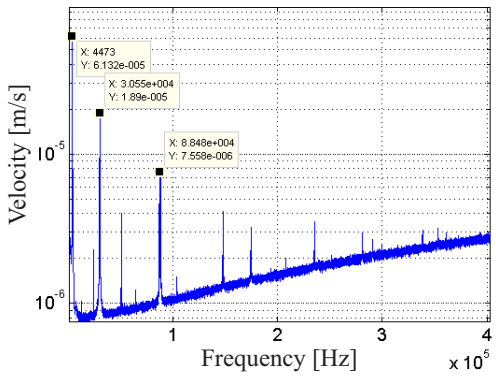

Figure 6: Mechanical response spectruc of a cantilever of area 1000x1000$\mu mT-$ and 5 μm thick. The first three resonances can be clearly observed.

As it can be observed, three clear resonances can be disguished, namely $f_1 = 4473Hz$, $f_2 = 30.55kHz$, $f_3 = 87.4kHz$. These will be the first three resonant modes of the structure.

4.2 Vibration mode selection

Figure 7 shows the circuit scheme used to implement the PDO. The excitation is composed of short pulses of voltage applied to the thermoelectric resistors. The MEMS position is detected through the Wheadstone bridge located in the cantilever. In this section, the cantilever that was measured was the one with an area of 1000x1000 μm^2 and 5μ thickness. The configurations predicted in Figures 3-4, and one more with $\sigma = 1, L = 15$, were used to selectively activate the first three resonances of this cantilever (sampling frequency $f_S = 138992$ Hz). In all these configurations the desired resonance is in the oscillation mode whereas the others are in anti-oscillation mode.

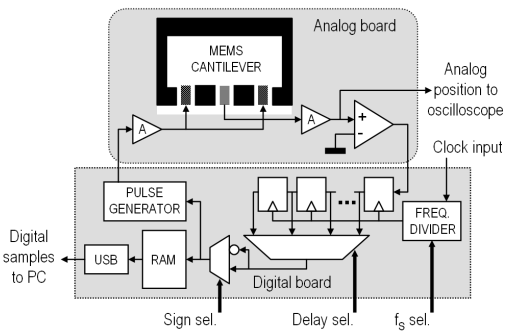

Figure 7: Circuit scheme used to implement the PDO to activate different resonances.

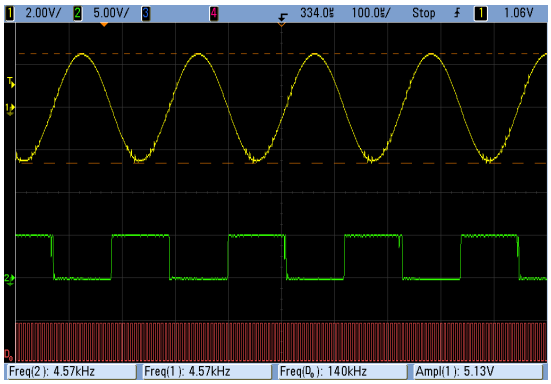

Figure 8: Oscilloscope screenshot showing the excitation of the first longitudinal mode of the 1000x1000 μm^2 and 5μ thickness cantilever, activated with a PDO working in the configuration of Figure 3 ($\sigma = 1, L = 4$), and a sampling frequency $f_S = 138992$ Hz. Oscillation frequency: $f_1 = 4.46kHz$

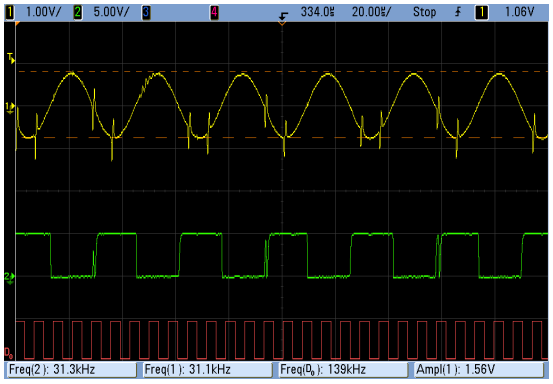

Figure 9: Oscilloscope screenshot showing the excitation of the second longitudinal mode of the 1000x1000 μm^2 and 5μ thickness cantilever, activated with a PDO working in the configuration of Figure 4 ($\sigma = 1, L = 13$), and a sampling frequency $f_S = 138992$ Hz. Oscillation frequency: $f_2 = 30.6kHz$

In all these Figures, the upper curve is the analog position of the MEMS cantilever, the medium curve is the bitstream at the output of the oscillator, and the bottom curve is the samping clock. The main contribution of the PDO structure is that the switching between modes is simply carried out by changing the number of delay blocks in the feedback loop (from $L = 4$ to $L = 13$ and $L = 15$ respectively).

Finally, with the scanning Doppler vibrometer, it was confirmed that each one of the resonances was indeed related to one of the first three longitudinal modes of the cantilever (see Figure 12). These figures show the shape of the vibrations excited in the MEMS with the three different feedback configurations applied to the PDO. They also show the spectra of the movement associated with each one of the configurations. As it can be clearly observed, the first three longitudinal modes are indeed excited. Note, that the oscillator is able to overcome the different amplitudes of the resonant modes that is appreciated in Figure 6. Note also, that each time a given mode is excited the oscillation amplitude of the others is much smaller (they are in the anti-oscillation region of the oscillator).

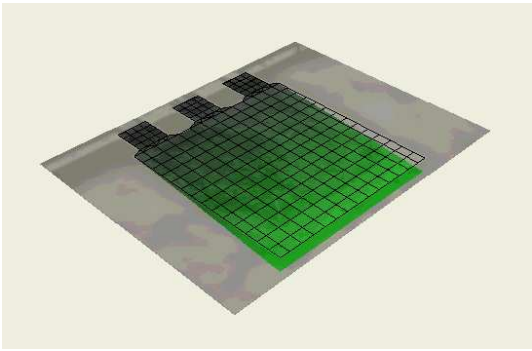

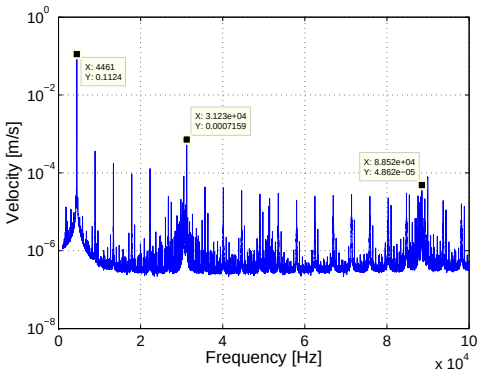

Figure 10: Measurement of the shape and spectrum of the first oscillation mode obtained with a scanning Doppler vibrometer.

The oscillation amplitudes for all the modes has been obtained from the vibrometer measurements. For the first one it is $d_{1max} = 13\mu m$, for the second $d_{2max} = 87$nm and finally for the third $d_{3max} = 23$nm.

One of the key points of PDOs is that we can retrieve the oscillation frequency directly from the bitstream. On the other hand, it is known that for sampling frequencies below the Nyquist limit, it is not possible to retrieve perfectly the oscillation frequency, but that frequency shifts can be easily monitored. This is what happens for example in the activation of the third resonance for the above cantilever, and the configurations chosen ($f_S = 138992$ Hz and resonant frequency $f_3 = 88.41kHz$). As it can be seen, $f_S \not> 2f_3$, and therefore we are in undersampling conditions. However, if we know beforehand the value of $r = \lfloor 2f_{res}/f_S \rfloor$, where $\lfloor\ a \rfloor$ is the largest integer less or equal to a, then it is possible to recover perfectly the oscillation frequency directly from the

bitstream:

$$f_D^* = \begin{cases} \left(\frac{r}{2} + f_D\right) f_S & \text{if} \quad r \quad \text{is even} \\ \left(\frac{r+1}{2} - f_D\right) f_S & \text{if} \quad r \quad \text{is odd} \end{cases} \tag{10}$$

It must be noted though that, even when the value of r is not exactly known, small shifts in the resonant frequency of the resonator (such as those when the resonator is used as a microbalance), can still be measured.

The main advantage of working below the Nyquist frequency may in the future be the activation of high frequency resonators. This fact, together with the activation of different modes mayt produce very high resonant frequencies. Thus, working below the Nyquist frequency may be a desired feature, because it may serve to simplify the associated sensing/actuating electronics.

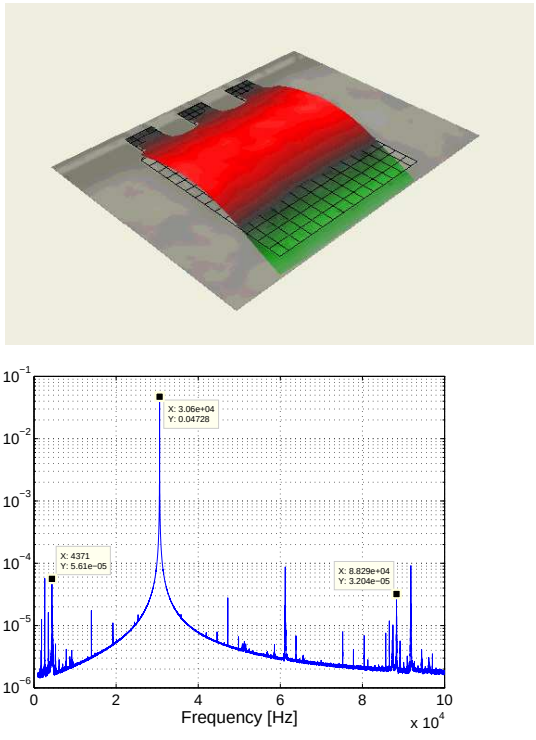

Figure 11: Measurement of the shape and spectrum of the second oscillation mode obtained with a scanning Doppler vibrometer.

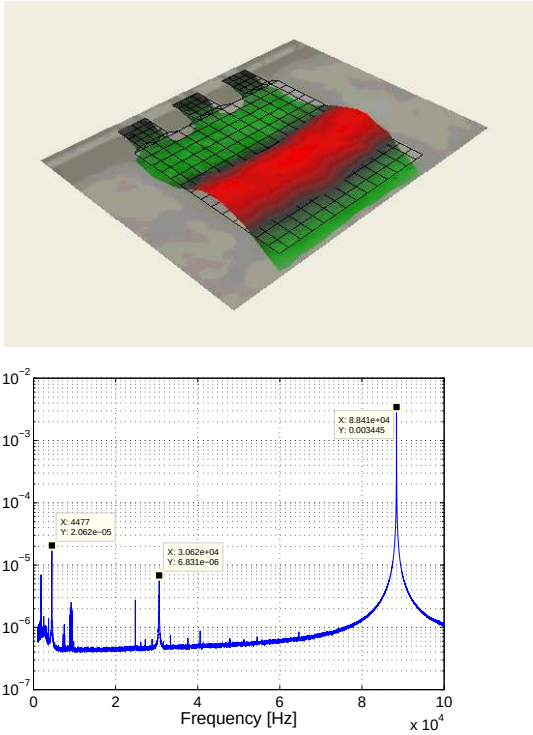

Figure 12: Measurement of the shape and spectrum of the third oscillation mode obtained with a scanning Doppler vibrometer.

5 Conclusions

In this paper we have shown it is possible to excite and control different modes of a MEMS resonator by simply changing some parameters on the feedback filter of the PDO structure. Numerical simulations have shown that the PDO system displays selective excitation of various spatial modes of the mechanical structure. Besides the parameters responsible for the output control such as the sampling frequency and the feedback filter, the output of the PDO depends on the position of the sensing/actuating system: its location enhances high-order modes and improve the sensitivity of the device. However, in the case when the sampling frequency is chosen in such a way that two or more modes are in the oscillation mode, the output of the circuit may depend on initial deformation of the beam. Extensive experimental measurements have been carried out and the final corroboration of the excitation of different resonant modes has been made with a scanning Doppler vibrometer.

Acknowledgements
This work was supported by the Spanish government through the TEC2007-67951/MIC, the DPI2009-07497 (both FEDER) projects and by Science Foundation Ireland.

References

[1] Zhang, W. and Turner, K. L., "Application of parametric resonance amplification in a single-crystal silicon micro-oscillator based mass sensor," *Sensors and Actuators A* **122**, 23–30 (2005).

[2] Spletzer, M., Raman, A., Wu, A. Q., and Xu, X., "Ultrasensitive mass sensing using mode localization in coupled microcantilevers," *Appl. Phys. Lett.* **88**, 254102 (2006).

[3] Sharos, L. B., Raman, A., Crittenden, S., and Reifenberger, R., "Enhanced mass sensing using torsional and lateral resonances in microcantilevers," *Appl. Phys. Lett.* **84**, 4638 (2004).

[4] Dohn, S., Sandberg, R., Svendsen, W., and Boisen, A., "Enhanced functionality of cantilever based mass sensors using higher modes," *Applied Physics Letters* **86**, 233501 (2005).

[5] Ghatkesar, M. K., Barwich, V., Braun, T., Ramseyer, J.-P., Gerber, C., Hegner, M., Lang, H. P., Drechsler, U., and Despont, M., "Higher modes of vibration increase mass sensitivity in nanomechanical cantilevers," *Nanotechnology* **18**, 445502 (2007).

[6] Domínguez, M., Pons-Nin, J., Ricart, J., Bermejo, A., Figueras Costa, E., and Morata, M., "Analysis of the $\Sigma - \Delta$ pulsed digital oscillator for MEMS," **52**, 2286–2297 (2005).

[7] Domínguez, M., Pons-Nin, J., Ricart, J., Bermejo, A., and Figueras Costa, E., "A novel $\Sigma - \Delta$ pulsed digital oscillator (PDO) for MEMS," **5**, 1379–1388 (2005).

[8] Domínguez, M., Pons-Nin, J., and Ricart, J., "General dynamics of pulsed digital oscillators," **55**, 2038–2050 (2008).

[9] Ricart, J., Pons, J., Domínguez, M., Rodríguez, A., Figueras, E., Gutiérrez, M. C. H. J., and Sayago, I., "Application of pulsed digital oscillators to volatile organic compounds sensing," *Sensors and Actuators B* **134**, 773–779 (2008).

[10] Blokhina, E., Pons, J., Ricart, J., Feely, O., and Dominguez, M., "Control of mems resonant modes with pulsed digital oscillators: Part 1," **in print**, – (2010).

ISBN 978-3-8007-3260-9